

Linear co-volume scheme for anisotropic curvature driven motions

Stefania Corsaro¹, Valentina De Simone¹, Angela Handlovičová²,
Karol Mikula², and Fiorella Sgallari³

¹ Center for Research on Parallel Computing and Supercomputers, CPS-CNR,
Complesso Universitario Monte S. Angelo, via Cintia, 80126 Napoli, Italy
{*stefania.corsaro, valentina.desimone*}@dma.unina.it

² Department of Mathematics, Slovak University of Technology, Radlinského 11,
813 68 Bratislava, Slovakia {*angela, mikula*}@vox.svf.stuba.sk

³ Department of Mathematics, University of Bologna, Piazza di Porta S. Donato
5, 40127 Bologna, Italy *sgallari@dm.unibo.it*

Summary. We introduce a linear semi-implicit complementary volume numerical scheme for solving level-set-like nonlinear diffusion equation arising in plane curve evolution driven by curvature and anisotropy. The scheme is L_∞ and $W^{1,1}$ stable and the efficiency is given by its linearity. Incomplete Cholesky preconditioners are used for computing arising linear systems in a fast way. Computational results related to anisotropic mean curvature motion in a plane are presented.

Key words: anisotropic mean curvature flow, level set equation, linear semi-implicit scheme, complementary volume method, preconditioners.

1 Introduction

The aim of this paper is to present a linear semi-implicit complementary volume numerical scheme for solving anisotropic curvature driven evolution of plane curves. We deal with discretization of the following nonlinear partial differential equation

$$u_t = \gamma(\theta)|\nabla u|\nabla \cdot \left(\frac{\nabla u}{|\nabla u|} \right), \quad (1)$$

where $u(t, x)$ is an unknown function defined in $Q_T \equiv I \times \Omega$, $I = [0, T]$ is a time interval, $\Omega \subset \mathbb{R}^2$ is a bounded domain with a Lipschitz continuous boundary, and $\theta = \angle\left(\frac{(\nabla u)^\perp}{|\nabla u|}, x_1\right)$ is the angle of the tangent to a level line of u and coordinate axis x_1 at point $x = (x_1, x_2)$ and time t . The equation is accompanied with zero Neumann boundary condition and initial conditions

$$\partial_\nu u = 0 \quad \text{on } I \times \partial\Omega, \quad (2)$$

$$u(0, x) = u^0(x) \quad \text{in } \Omega. \quad (3)$$

We assume that

$$0 < c \leq \gamma \leq C < \infty, \quad (4)$$

i.e., $\gamma(\theta)$ is a bounded strictly positive function representing anisotropy. Since $\frac{\nabla u}{|\nabla u|}$ gives the unit normal vector \mathbf{N} to a level line of a smooth function u with nonzero

gradient and $\nabla \cdot \mathbf{N}$ gives the curvature of this level line, equation (1) represents the so-called level set formulation ([22, 26]) of the anisotropic curve shortening flow problem (see e.g. [2, 19, 12, 20])

$$v = \gamma(\theta)k, \quad (5)$$

where normal velocity v of the evolving curve Γ (e.g., a closed level line of u considered above) at any point $x \in \Gamma$ is proportional to its curvature k at the point x multiplied by $\gamma(\theta)$ with θ given at x . The equations of the form (5) appear within a large variety of applied problems. They can be often found in the material science, anisotropic dynamics of phase boundaries in thermomechanics, in modeling of flame front propagation, in combustion, in computational geometry, robotics, semiconductors industry, etc. They also have a special importance in the image processing and computer vision. They are capable to model the so-called morphological image and shape multiscale analysis studied by Alvarez, Guichard, Lions and Morel [1]. An image isophote corresponding to a level line of the image intensity u is driven by (5) in the level set formulation (1) and the image is correspondingly smoothed in a morphologically invariant way [1, 15]. Examples of anisotropic-like models can be found in the image segmentation (see e.g. [6]); anisotropy can help to preserve corners of the segmented objects. For an overview of various aspects and applications of the equation (5) we refer to recent books by Sethian and Sapiro [27, 24].

Another formulation of anisotropic curvature driven motion is also used (see e.g. [3, 25, 12])

$$v = k_\alpha, \quad (6)$$

with k_α the so-called anisotropic curvature, where $\alpha : S^1 \rightarrow \mathbb{R}$, $\alpha > 0$, is an anisotropic surface energy weight function depending on the normal vector \mathbf{N} to the curve. In the case of curves, one can take $\alpha(\mathbf{N}) = \tilde{\alpha}(\theta)$, then (6) corresponds to $v = (\tilde{\alpha} + \tilde{\alpha}'')k$ and the relation $\gamma = \tilde{\alpha} + \tilde{\alpha}''$ is seen ([25]). By the method presented in this paper, we can thus compute evolution for anisotropic weight function α with strictly convex Frank diagrams (polar graph of $1/\alpha$).

Provided $\gamma \equiv 1$, (1) is called the *level set equation* proposed by Osher and Sethian ([22], [26]) for computation of moving fronts. The existence of its solution in a viscosity sense was given in [7, 14]. For the numerical solution Osher and Sethian proposed an explicit time stepping algorithm based on up-wind schemes for Hamilton-Jacobi equations. However, since (1) is a second order (degenerate) parabolic equation and nonlinearities depend on ∇u (and thus they are piecewise constant on triangles in case of piecewise linear functions given on a triangulation), the linear finite element ([8, 9, 10, 11, 25]) or complementary volume methods ([28, 16]) are also well suited for numerical solution. Taking time discretization in a semi-implicit way, such methods are unconditionally stable, simply implemented and, using state-of-the-art of the preconditioned linear algebra solvers one can achieve fast CPU times. Besides the level set formulation (1) of the geometrical equation (5), the phase-field approximations (see e.g. [21, 3, 13, 5, 4] and references there) and direct methods [19, 12, 20] have been developed to model and compute anisotropic curve evolution.

In this paper we extend the linear semi-implicit co-volume scheme given in [16] (for selective image smoothing) to new class of applications, namely to solve anisotropic curve shortening in the level set formulation (1). In Section 2 we present

the scheme and give some of their properties. In Section 3 we discuss computational results.

2 Linear semi-implicit co-volume scheme

In this section we present semi-implicit complementary volume discretization of the problem given by (1). We discretize the time interval $[0, T]$. Choosing $N \in \mathbb{N}$ we have given the length of a uniform discrete time step $\tau = \frac{T}{N}$. We replace the time derivative in (1) by backward difference and the nonlinear terms of equations are treated from the previous time step while the linear ones are considered on the current time level - this means semi-implicitness of the method. Equation (1) is not written in divergence form. For partial derivatives of second order, as it is usual in variational methods, we would like to use integration by parts or divergence theorem to get integral formulation. Thus, first we move the terms in front of divergence to time derivative and then write semi-implicit discretization of (1) in time.

Semi-discrete linear scheme for solving equation (1): Let $N \in \mathbb{N}$, $\tau = \frac{T}{N}$ be fixed numbers and u^0 be given by (3). For every $n = 1, \dots, N$, we look for a function u^n , solution of the equation

$$\frac{1}{\gamma^{n-1} |\nabla u^{n-1}|} \frac{u^n - u^{n-1}}{\tau} - \nabla \cdot \left(\frac{\nabla u^n}{|\nabla u^{n-1}|} \right) = 0, \quad (7)$$

where $\gamma^{n-1} = \gamma(\theta^{n-1})$, $\theta^{n-1} = \angle\left(\frac{(\nabla u^{n-1})^\perp}{|\nabla u^{n-1}|}, x_1\right)$. Walkington in [28] first studied a co-volume scheme for curvature driven motion (with $\gamma \equiv 1$). He used an interesting approximation of degenerate diffusion term

$$\frac{1}{|\nabla u^{n-1}|} \frac{u^n - u^{n-1}}{\tau} - 2 \nabla \cdot \left(\frac{\nabla u^n}{|\nabla u^n| + |\nabla u^{n-1}|} \right) = 0 \quad (8)$$

taking average of gradients from previous and current time step in denominator of divergence term in order to get important $W^{1,1}$ estimate, i.e. estimate on decay of total variation of semi-discrete solutions. It is a basic property of the flow by mean curvature and of a solution of level set equation as well so a numerical approximation should respect this fact. Following [28] one can multiply (8) by $u^n - u^{n-1}$ and integrate it over Ω . Then using integration by parts and zero Neumann boundary conditions one gets

$$\int_{\Omega} \frac{(u^n - u^{n-1})^2}{\tau |\nabla u^{n-1}|} dx + 2 \int_{\Omega} \frac{\nabla u^n \cdot (\nabla u^n - \nabla u^{n-1})}{|\nabla u^{n-1}| + |\nabla u^n|} dx = 0. \quad (9)$$

Using the relation

$$2a(a - b) = a^2 - b^2 + (a - b)^2 \quad (10)$$

where a, b are arbitrary real numbers, and by a simple manipulations related to the sum in denominator one gets

$$\begin{aligned}
& \int_{\Omega} \frac{(u^n - u^{n-1})^2}{\tau |\nabla u^{n-1}|} dx + \int_{\Omega} \frac{|\nabla u^n|^2 - |\nabla u^{n-1}|^2}{|\nabla u^{n-1}| + |\nabla u^n|} dx + \\
& + \int_{\Omega} \frac{|\nabla u^n - \nabla u^{n-1}|^2}{|\nabla u^{n-1}| + |\nabla u^n|} dx = \int_{\Omega} \frac{(u^n - u^{n-1})^2}{\tau |\nabla u^{n-1}|} dx + \\
& + \int_{\Omega} \frac{|\nabla u^n - \nabla u^{n-1}|^2}{|\nabla u^{n-1}| + |\nabla u^n|} dx + \left(\int_{\Omega} |\nabla u^n| dx - \int_{\Omega} |\nabla u^{n-1}| dx \right) = 0
\end{aligned} \tag{11}$$

which means that

$$\|\nabla u^n\|_{L_1(\Omega)} \leq \|\nabla u^{n-1}\|_{L_1(\Omega)} \tag{12}$$

and by recursion

$$\|\nabla u^n\|_{L_1(\Omega)} \leq \|\nabla u^0\|_{L_1(\Omega)}, \quad 1 \leq n \leq N, \tag{13}$$

which is $W^{1,1}$ stability property of Walkington's nonlinear co-volume scheme. One could adjust the previous scheme (8) to the anisotropic situation. But, the ‘‘implicit’’ time discretization used in (8) leads (after any spatial discretization) to solving of nonlinear system of equations in each discrete time step which is rather non-efficient approach. In order to have convergence, which is however very slow, one has to use fixed point-like nonlinear iterations; faster possibilities like Newton's method has no guarantee to converge ([28]) and are also rather complicated from implementation point of view. In spite of that, we can get decay of total variation of solutions on subsequent time steps also for scheme (7) which is much more simple and efficient since it is linear. As linear, it allows to use fast preconditioned iterative solvers at every time level with fast CPU times. In order to get (13) for our scheme let us multiply (7) by $u^n - u^{n-1}$ and integrate it over Ω . Using (10) we get

$$\int_{\Omega} \frac{(u^n - u^{n-1})^2}{\tau \gamma^{n-1} |\nabla u^{n-1}|} dx + \frac{1}{2} \int_{\Omega} \frac{|\nabla u^n|^2 - |\nabla u^{n-1}|^2 + |\nabla u^n - \nabla u^{n-1}|^2}{|\nabla u^{n-1}|} dx = 0. \tag{14}$$

Since

$$|\nabla u^n - \nabla u^{n-1}|^2 = (|\nabla u^n| - |\nabla u^{n-1}|)^2 + \left(\frac{\nabla u^n}{|\nabla u^n|} - \frac{\nabla u^{n-1}}{|\nabla u^{n-1}|} \right)^2 |\nabla u^n| |\nabla u^{n-1}| \tag{15}$$

we get

$$\begin{aligned}
& \int_{\Omega} \frac{(u^n - u^{n-1})^2}{\tau \gamma^{n-1} |\nabla u^{n-1}|} dx + \frac{1}{2} \int_{\Omega} \frac{|\nabla u^n|^2 - |\nabla u^{n-1}|^2 - (|\nabla u^n| - |\nabla u^{n-1}|)^2}{|\nabla u^{n-1}|} dx \\
& + \int_{\Omega} \frac{(|\nabla u^n| - |\nabla u^{n-1}|)^2}{|\nabla u^{n-1}|} dx + \frac{1}{2} \int_{\Omega} \left(\frac{\nabla u^n}{|\nabla u^n|} - \frac{\nabla u^{n-1}}{|\nabla u^{n-1}|} \right)^2 |\nabla u^n| dx = 0.
\end{aligned}$$

Due to positivity of other terms we get for the second one

$$\int_{\Omega} \frac{|\nabla u^n| |\nabla u^{n-1}| - |\nabla u^{n-1}|^2}{|\nabla u^{n-1}|} dx \leq 0 \tag{16}$$

which gives desired stability property

$$\|\nabla u^n\|_{L_1(\Omega)} \leq \|\nabla u^{n-1}\|_{L_1(\Omega)}. \tag{17}$$

In order to derive a fully discrete scheme, let us assume that we have given a triangulation \mathcal{T}_h (which has no interior angle larger than $\pi/2$) of the domain Ω . We construct a dual mesh which consist of cells V_i (called also complementary volumes, control volumes or co-volumes) associated with the i th node of triangulation \mathcal{T}_h , $i = 1, \dots, M$. The co-volume V_i is bounded by the lines that bisect and are perpendicular to the edges emanating from the node. We will denote the edge of \mathcal{T}_h connecting the i th node to the j th by σ_{ij} and its length by h_{ij} . We denote by \mathcal{E}_{ij} the set of simplices having σ_{ij} as an edge, i.e., $\mathcal{E}_{ij} = \{T \in \mathcal{T}_h | \sigma_{ij} \subset T\}$. Let e_{ij} denote the co-edge that is the perpendicular bisector of σ_{ij} and x_{ij} be a point of intersection of e_{ij} and σ_{ij} . For each $T \in \mathcal{E}_{ij}$ let c_{ij}^T be the length of the portion of e_{ij} that is in T , i.e., $c_{ij}^T = |e_{ij} \cap T|$. Let \mathcal{N}_i be the set of simplices that have the i th node as a vertex, and for each node of \mathcal{T}_h let C_i denote the set of nodes connected to the i th node by an edge. Given a triangulation \mathcal{T}_h , we define the set $V_h \subset V$ of piecewise linear finite elements, i.e., $V_h = V_h(\mathcal{T}_h) := \{v \in C^0(\bar{\Omega}) | v|_T \in \mathcal{P}_1 \text{ for all } T \in \mathcal{T}_h\}$. For any $v_h \in V_h$ we will use the notation $v_i := v_h(x_i)$ where x_i is i th node of triangulation. Let $u_h^0 = I_h(u^0) \in V_h(\mathcal{T}_h)$ be the nodal interpolant of u^0 , the initial function for the complementary volume method.

In order to derive complementary volume spatial discretization we integrate (7) over a co-volume V_i

$$\int_{V_i} \frac{u^n - u^{n-1}}{\gamma^{n-1} |\nabla u^{n-1}|_T} dx = \int_{V_i} \nabla \cdot \left(\frac{\nabla u^n}{|\nabla u^{n-1}|} \right) dx. \quad (18)$$

For the right hand side using divergence theorem we get

$$\int_{V_i} \nabla \cdot \left(\frac{\nabla u^n}{|\nabla u^{n-1}|} \right) dx = \int_{\partial V_i} \frac{1}{|\nabla u^{n-1}|} \frac{\partial u^n}{\partial \nu} ds = \sum_{j \in C_i} \int_{e_{ij}} \frac{1}{|\nabla u^{n-1}|} \frac{\partial u^n}{\partial \nu} ds. \quad (19)$$

If $u_h^n \in V_h(\mathcal{T}_h)$ is continuous piecewise linear function on triangulation \mathcal{T}_h and we have denoted $u_i = u_h(x_i)$ its nodal values then

$$\sum_{j \in C_i} \int_{e_{ij}} \frac{1}{|\nabla u_h^{n-1}|} \frac{\partial u_h^n}{\partial \nu} ds = \sum_{j \in C_i} \left(\sum_{T \in \mathcal{E}_{ij}} \frac{c_{ij}^T}{|\nabla u_T^{n-1}|} \right) \frac{u_j^n - u_i^n}{h_{ij}} \quad (20)$$

where ∇u_T^{n-1} denotes the constant gradient vector of u_h^{n-1} in the simplex T and $|\nabla u_T^{n-1}|$ is its absolute value. In the complementary volume method we approximate the left hand side of (18) by

$$\frac{|V_i|(u_i^n - u_i^{n-1})}{\tau \gamma_i^{n-1} |\nabla u_i^{n-1}|} \quad (21)$$

where we have taken weighted averages of the constant quantities on triangles intersecting co-volume V_i , namely

$$\nabla u_i^{n-1} \approx \sum_{T \in \mathcal{N}_i} \frac{|T \cap V_i|}{|V_i|} \nabla u_T^{n-1}, \quad (22)$$

$$|\nabla u_i^{n-1}| \approx \sum_{T \in \mathcal{N}_i} \frac{|T \cap V_i|}{|V_i|} |\nabla u_T^{n-1}|, \quad (23)$$

$$\theta_i^{n-1} \approx \angle\left(\frac{(\nabla u_i^{n-1})^\perp}{|\nabla u_i^{n-1}|}, x_1\right), \quad \gamma_i^{n-1} = \gamma(\theta_i^{n-1}). \quad (24)$$

If we denote by

$$b_i^{n-1} = \frac{|V_i|}{\gamma_i^{n-1} |\nabla u_i^{n-1}|}, \quad (25)$$

$$a_{ij}^{n-1} = \frac{1}{h_{ij}} \sum_{T \in \mathcal{E}_{ij}} \frac{c_{ij}^T}{|\nabla u_T^{n-1}|}, \quad (26)$$

we can write **linear fully discrete complementary volume scheme for solving equation (1)**: For $n = 1, \dots, N$ we look for $u_i^n, i = 1, \dots, M$ satisfying

$$b_i^{n-1}(u_i^n - u_i^{n-1}) + \tau \sum_{j \in C_i} a_{ij}^{n-1}(u_i^n - u_j^n) = 0. \quad (27)$$

By the above construction, it is not difficult to see that system (27) gives a symmetric positive definite M-matrix with diagonal dominance.

Using nonnegativeness of b_i^{n-1}, a_{ij}^{n-1} we can get L_∞ -stability estimate for fully discrete scheme (27) in the form

$$\min u_i^0 \leq \min u_i^n \leq \max u_i^n \leq \max u_i^0, \quad 1 \leq n \leq N \quad (28)$$

which means

$$\|u_h^n\|_{L_\infty(\Omega)} \leq \|u_h^0\|_{L_\infty(\Omega)}, \quad 1 \leq n \leq N. \quad (29)$$

To see (28), let us rewrite (27) in the form

$$u_i^n + \frac{\tau}{b_i^{n-1}} \sum_{j \in C_i} a_{ij}^{n-1}(u_i^n - u_j^n) = u_i^{n-1} \quad (30)$$

and let $\max u_h^n = \max(u_1^n, \dots, u_M^n)$ be achieved in the i th node. Then the whole second term on the left hand side is nonnegative and thus value $u_i^n \leq u_i^{n-1} \leq \max(u_1^{n-1}, \dots, u_M^{n-1})$. In the same way we can prove the relations for minima.

Until now, we have not solved the problem of possible zero gradients in denominators of the scheme (7) or (27). To prevent such situation we can use Evans-Spruck type regularization and consider

$$|\nabla u|_\varepsilon = \sqrt{\varepsilon + |\nabla u|^2} \quad (31)$$

instead of $|\nabla u|$ everywhere in the schemes (7) and (27) or just when $|\nabla u|$ is vanishing. The stability results which we derived so far formally, i.e. L_∞ and $W^{1,1}$ estimates (28) and (17), are valid for such regularization of the fully discrete scheme (27). Since γ fullfils (4), to that goal one can use the results from [16]. Moreover they do not depend on regularization parameter ε thus we can pass to the limit and understand solution of (27) in a generalized sense as in [16].

3 Numerical experiments

This section is devoted to discussion on numerically computed examples and includes also discussion on computational efficiency of iterative solvers used in our

semi-implicit scheme (27). In all presented examples we have used $\varepsilon = 10^{-6}$, $\tau = 0.001$, and we use simple uniform grid with spatial step size $h = 0.01$ where every square is divided into two triangles in order to have triangulation \mathcal{T}_h . The dual mesh then consists of shifted squares. We take signed distance (see [27]) to initial curve as initial condition $u^0(x)$. We visualize evolving zero level line of u corresponding to evolving curve at discrete time moments.

In Figures 1 and 2 we present computations with four-fold anisotropy given by $\gamma(\theta) = 1 - 0.8 \cos(4\theta)$. First, the evolution of unit circle is computed and visualized (every 100th time step) in Figure 1 left. The evolution precisely coincides with solution given by conceptually different methods based on a porous-media-like formulation for which convergence to weak solution is known [19] and with a method based on discretization of the intrinsic heat equation [20]. We plot by solid lines numerical solution given by co-volume scheme (27) and by points the solution given by direct methods (both give undistinguished discrete curve representations). In the figure, one can see minor error in extinction of the curve; computed extinction time is 0.503, while the exact one is 0.5. Next we use the method (27) for evolution of initial nonconvex curve (five-petal). In Figure 1 right we visualize every 20th time step until $T = 0.2$. The comparison with direct method [20] is of similar precision to those presented in the left.

In the computations given in Figure 2 we accompany the curve shortening (5) with an external constant driving force F . Such model represents the Angenent-Gurtin approach to solid-liquid planar interface motion for perfect conductors [2]. We consider geometrical equation of the form

$$v = \gamma(\theta)k + F. \quad (32)$$

We present computations with negative F (driving a curve to expand) and we plot both solutions every 20th time step until $T = 0.2$. In this case, the only modification of the scheme (27) consists in nonzero right hand side given now by $\frac{F\tau|V_i|}{\gamma_i}$. In Figure 3 we plot evolutions of two nonconvex curves (four-petals) using anisotropies $\gamma(\theta) = 1 - 0.98 \cos(3\theta)$ (left) and $\gamma(\theta) = 1 - 0.95 \cos(6\theta)$ (right) and we visualize every 20th time step until $T = 0.2$ (left), $T = 0.3$ (right), respectively.

An efficient implementation of semi-implicit scheme (27) requires fast solution of the large linear systems. We have focused on the preconditioned conjugate gradient (PCG) method because the coefficient matrices are symmetric positive definite M-matrix with diagonal dominance. Incomplete Cholesky factorization (ICF) has been a general way for obtaining a preconditioner and a good experience have been done in the PDE-image processing environment in [16]. A key issue in ICF is to choose the sparsity pattern S . Many methods have been proposed for finding a good S . The first ICF proposed by Meijerink and van der Vorst [18] kept the sparsity pattern of the original matrix. Another popular ICF method is based on the drop tolerance approach in which nonzeros are included in the incomplete factor when they are larger than some threshold parameter. Therefore, the memory requirements are unpredictable. Many variants and detailed descriptions of the algorithms can found in Saad's book [23]. We have implemented Lin and Moré's idea that allows memory saving. The incomplete factor is calculated column by column. After a column is obtained, only the p largest (in magnitude) elements are stored back to the factor.

In Table 1 we report CPU times and the number of matrix-vector multiplications used to obtain convergence in the solution of the linear system in one time step of

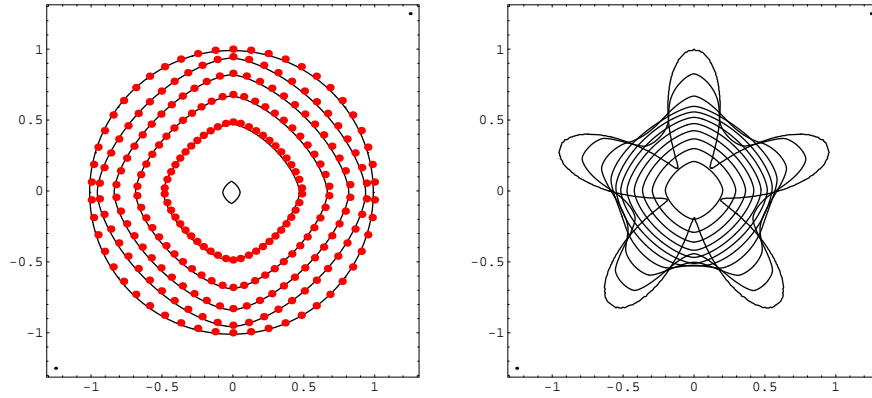


Fig. 1. Anisotropic curvature driven evolution of the unit circle (left) and initial nonconvex curve (right) under the same anisotropy.

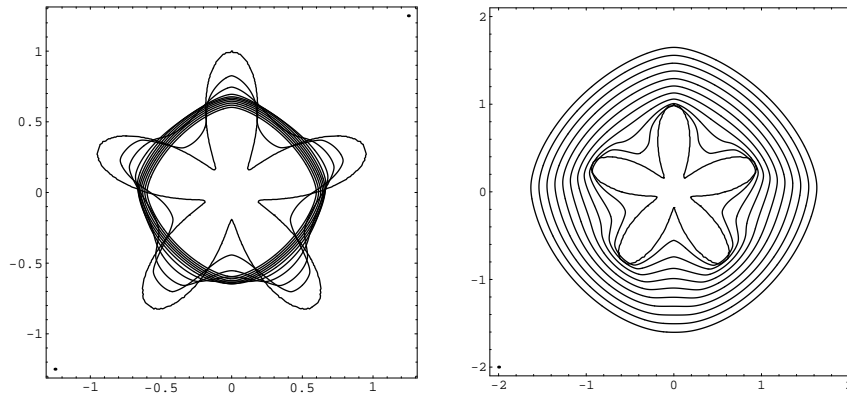


Fig. 2. Anisotropic curvature driven evolution of the initial nonconvex curve with a constant driving force $F = -1$ (left), $F = -5$ (right).

the semi-implicit scheme according to the level of fill-in p . As stopping criterion we have used $\|r^k\|_2 \leq tol \|r^0\|_2$ with tolerance $tol = 10^{-6}$, where $\|\cdot\|_2$ means discrete L_2 norm and r^k is residual in k th iteration. In dependence on p we report CPU time for construction of ICF preconditioner, CPU time for solving the system by PCG method, number of PCG iterations and total CPU time for one time step which includes also construction of coefficients for the system (27). The computations were done on Pentium II (800 MHz) with Linux operating system.

References

1. Alvarez, L., Guichard, F., Lions, P.L., Morel, J.M. (1993): Axioms and Fundamental Equations of Image Processing, Arch. Rat. Mech. Anal., **123**, 200–257

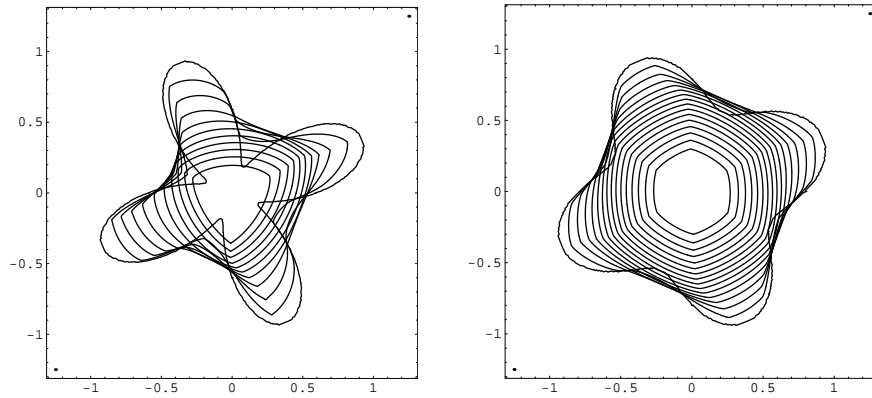


Fig. 3. Anisotropic curvature driven evolution of the initial nonconvex curves with three-fold (left) and six-fold (right) anisotropies.

Table 1. Behaviour of the preconditioned conjugate gradient solver at one time step of the semi-implicit scheme with 250×250 spatial discrete points

p -level of fill-in	0	2	4	6	8	10	20
Construction of preconditioner (sec)	0.21	0.29	0.37	0.51	0.60	0.71	1.39
CPU time of PCG solver (sec)	2.63	1.6	1.27	1.10	1.04	0.94	0.81
# PCG iterations	24	13	9	7	6	5	3
total CPU time in one time step (sec)	3.55	2.59	2.34	2.30	2.34	2.34	2.9

2. S.B.Angenent, S.B., Gurtin, M.E. (1989): Multiphase thermomechanics with an interfacial structure 2. Evolution of an isothermal interface, *Arch. Rat. Mech. Anal.*, **108**, 323–391
3. Bellettini, G., Paolini, M. (1996): Anisotropic motion by mean curvature in the context of Finsler geometry, *Hokkaido Math. J.*, **25**, 537–566
4. Beneš, M. (2000): Anisotropic phase-field model with focused latent-heat release, In *Proceedings on Free Boundary Problems, Theory and Applications. GAKUTO Int. Series, Vol. 14*, Chiba, 18–30
5. Beneš, M., Mikula, K. (1998): Simulations of anisotropic motion by mean curvature - comparison of phase field and sharp interface approaches, *Acta Math. Univ. Comenianae*, **67**, 17–42
6. Caselles, V., Kimmel, R., Sapiro, G. (1997): Geodesic active contours, *International Journal of Computer Vision*, **22**, 61–79.
7. Chen, Y.-G., Giga, Y., Goto, S. (1991): Uniqueness and existence of viscosity solutions of generalized mean curvature flow equation, *J. Diff. Geom.*, **33**, 749–786
8. Deckelnick, K., Dziuk, G. (1995): Convergence of a finite element method for non-parametric mean curvature flow, *Numer. Math.*, **72**, 197–222
9. Deckelnick, K., Dziuk, G. (1999): Discrete anisotropic curvature flow of graphs, *Mathematical Modelling and Numerical Analysis*, **33**, 1203–1222

10. Deckelnick, K., Dziuk, G. (2000): Error estimates for a semi-implicit fully discrete finite element method for the mean curvature flow of graphs, *Interfaces and Free Boundaries*, **2**, 341–359
11. Deckelnick, K., Dziuk, G. (2000): A fully discrete numerical scheme for weighted mean curvature flow, Preprint Math. Fak. Freiburg, Nr. 30/2000
12. Dziuk, G. (1999): Discrete anisotropic curve shortening flow, *SIAM J. Numer. Anal.*, **36**, 1808–1830
13. Elliott, C.M., Paolini, M., Schätzle, R. (1996): Interface estimates for the fully anisotropic Allen–Cahn equation and anisotropic mean curvature flow, *Mathematical Models and Methods in Applied Sciences*, **6**, 1103–1118
14. Evans, L.C., Spruck, J. (1991): Motion of level sets by mean curvature I, *J. Diff. Geom.*, **33**, 635–681
15. Handlovičová, A., Mikula, K., Sarti, A. (1999): Numerical solution of parabolic equations related to level set formulation of mean curvature flow, *Computing and Visualization in Science*, **1**, 179–182
16. Handlovičová, A., Mikula, K., Sgallari, F. (2001): Semi-implicit complementary volume scheme for solving level set like equations in image processing and curve evolution, *Numer. Math.*, DOI 10.1007/s002110100374
17. Lin, C.-J., Moré, J.J. (1999): Incomplete Cholesky factorizations with limited memory, *SIAM J. Sci. Comput.*, **21**, 24–45
18. Meijerink, J.A., van der Vorst, H.A. (1977): An iterative solution method for systems of which the coefficient matrix is a symmetric M-matrix, *Math. Comp.*, **31**, 148–162
19. Mikula, K., Kačur, J. (1996): Evolution of convex plane curves describing anisotropic motions of phase interfaces, *SIAM J. Sci. Comput.*, **17**, 1302–1327
20. Mikula, K., Ševčovič, D. (2001): Evolution of plane curves driven by a nonlinear function of curvature and anisotropy, *SIAM J. Appl. Math.*, **61**, 1473–1501
21. Nochetto, R., Paolini, M., Verdi, C. (1993): Sharp error analysis for curvature dependent evolving fronts, *Mathematical Models and Methods in Applied Sciences*, **3**, 711–723.
22. Osher, S., Sethian, J. (1988): Front propagating with curvature dependent speed: algorithms based on the Hamilton- Jacobi formulation, *J. Comput. Phys.*, **79** 12–49
23. Saad, Y. (1996): Iterative methods for sparse linear systems. PWS Publ. Comp.
24. Sapiro G. (2001): Geometric Partial Differential Equations and Image Processing. Cambridge University Press
25. Schmidt, A. (1998): Approximation of crystalline dendrite growth in two space dimensions, *Acta Math. Univ. Comenianae*, **67**, 57–68
26. Sethian, J.A. (1990): Numerical algorithm for propagating interfaces: Hamilton-Jacobi equations and conservation laws, *J. Diff. Geom.* **31** 131–161
27. Sethian, J.A. (1999): Level Set Methods and Fast Marching Methods. Evolving Interfaces in Computational Geometry, Fluid Mechanics, Computer Vision, and Material Science. Cambridge University Press
28. Walkington, N.J. (1996): Algorithms for computing motion by mean curvature, *SIAM J. Numer. Anal.*, **33**, 2215–2238